Journal of Avian Biology 43: 297–310, 2012
doi: 10.1111/j.1600-048X.2012.05474.x
© 2012 The Authors. Journal of Avian Biology © 2012 Nordic Society Oikos
Subject Editor: Staffan Bensch. Accepted 9 March 2012

Pleistocene climate changes shaped the divergence and demography of Asian populations of the great tit *Parus major*: evidence from phylogeographic analysis and ecological niche models

Na Zhao, Chuanyin Dai, Wenjuan Wang, Ruiying Zhang, Yanhua Qu, Gang Song, Kai Chen, Xiaojun Yang, Fasheng Zou and Fumin Lei

N. Zhao, C. Dai, W. Wang, R. Zhang, Y. Qu, G. Song, K. Chen and F. Lei (leifm@ioz.ac.cn), Key Laboratory of Zoological Systematics and Evolution, Inst. of Zoology, Chinese Academy of Sciences, Beijing 100101, China. CD, WW and RZ also at: Graduate Univ. of Chinese Academy of Sciences, Beijing 100049, China. – X. Yang, State Key Laboratory of Genetic Resources and Evolution, Kunming Inst. of Zoology, Chinese Academy of Sciences, Kunming 650224, China. – F. Zou, Guangdong Provincial Public Laboratory of Wild Animal Conservation and Management, South China Inst. of Endangered Animals, Guangzhou 510260, China.

Different scales and frequencies of glaciations developed in Europe and Asia during the Pleistocene. Because species' responses to climate change are influenced by interactive factors including ecology and local topography, the pattern and tempo of species diversification may vary significantly across regions. The great tit *Parus major* is a widespread Eurasian passerine with a range that encircles the central Asian desert and high-altitude areas of the Tibetan Plateau. A number of genetic studies have assessed the effect of paleo-climate changes on the distribution of the European population. However, none have comprehensively addressed how paleo-climate change affected the distribution of the great tit in China, an apparent hotspot of *P. major* subspecific diversity. Here, we describe likely paleo-climatic effects on *P. major* populations in China based on a combination of phylogeography and ecological niche models (ENMs). We sequenced three mitochondrial DNA markers from 28 populations (213 individuals), and downloaded 112 sequences from outside its Chinese range. As the first step in clarifying the intra-specific relationships among haplotypes, we attempted to clarify the divergence and demography of populations in China. Phylogeographic analysis revealed that *P. major* is comprised of five highly divergent clades with geographic breaks corresponding to steep mountains and dry deserts. A previously undescribed monophyletic clade with high genetic diversity, stable niches and a long and independent evolutionary history was detected in the mountainous areas of southwest China. The estimated times at which these clades diverged was traced back to the Early-Middle Pleistocene (2.19–0.61 mya). Contrary to the post-LGM (the Last Glacial Maximum) expansion of European populations, demographic history indicates that Asian populations expanded before the LGM after which they remained relatively stable or grew slowly through the LGM. ENMs support this conclusion and predict a similar distribution in the present and the LGM. Our genetic and ecological results demonstrate that Pleistocene climate changes shaped the divergence and demography of *P. major* in China.

Climate oscillations in the Pleistocene have had profound effects on the demography and genetic diversity of many extant species (Hewitt 1996, 2000, 2004, Avise 2000). Because species' responses to climate change are influenced by interactive factors, including ecology and local topography, the pattern and tempo of diversification may differ between taxa and vary significantly across regions (Hewitt 1996, 2000, 2004, Avise 2000). In the Pleistocene, different regions went through different scales and frequencies of glaciations. In Europe, the Pleistocene ice sheet covered the continent to approximately 52°N during major glaciations (Taberlet et al. 1998). In contrast, China was not glaciated during the Pleistocene (Williams et al. 1998) and had a relatively mild Quaternary climate (Weaver et al. 1998). Therefore, while severe climatic oscillations in Europe forced many species to either move, adapt or go extinct (Avise 2000, Hewitt 2000, 2004), China's relatively mild Pleistocene climate probably allowed many species to remain in situ and to undergo less dramatic population fluctuations or evolutionary change. In contrast to its relative climatic stability, China is characterized by topological complexity. The mountainous areas of southwest China, surrounding the southeastern flanks of the Tibetan Plateau, have perhaps the most complex topography on Earth. These mountains rose rapidly with the uplift of the Tibetan Plateau (Patriat and Achache 1984, Tapponnier et al. 2001, Royden et al. 2008). However, even during the Pleistocene, only land above 2000 m a.s.l. was glaciated (Li et al. 1991, Zhou et al. 2006). Therefore, compared to the extremes experienced by their European counterpart, China's relatively mild

Pleistocene climate and diverse local-topography would be expected to have had quite different effects on species' distribution, divergence and historical demography.

Previous studies of east Asian avifauna have highlighted genetic differentiation, unusual historical demography and the existence of multiple refugia during glacial periods (Johansson et al. 2007, Zou et al. 2007, Li et al. 2009, Qu and Lei 2009, Song et al. 2009, Liu et al. 2010, Qu et al. 2011). Although the consensus is that the last glacial maximum (LGM) had a limited effect on species' distribution and demography (Li et al. 2009, Dai et al. 2011, Qu et al. 2011), these studies focused primarily on endemic species in south China or southwest China. Additional research on a species with a Pan-Eurasian distribution is therefore required to confirm the generality of existing hypotheses on how Pleistocene climate change affected species diversification and demography.

The great tit *Parus major* is a widespread passerine bird with a range that encircles the central Asian desert and high-altitude areas of the Tibetan Plateau. Although subspecies classification has been complicated by the species' high morphological variability, they can be generally classified into four subspecies groups: *major*, *minor*, *cinereus* and *bokharensis* (Stegmann 1931, Eck and Piechocki 1977, Eck and Martens 2006). Molecular data indicate that the relationships between these four groups are ((*major*, *bokharensis*), (*minor*, *cinereus*)) (Kvist et al. 2003, Päckert et al. 2005, Zink 2005). Detailed genetic studies have been done on European populations (Kvist et al. 2003, 2007, Päckert et al. 2005, Pavlova et al. 2006). These studies revealed that Pleistocene glacial cycles had profound impacts on great tit distribution in Europe and that great tit populations experienced post-glacial expansion from southern refugia to northern regions (Kvist et al. 2003). However, although China is an apparent hotspot of *P. major* subspecies diversity, there has been no investigation of its phylogeography in China. Seven subspecies of *P. major* occur in China: *P. m. kapustini* in the extreme northwest and northeast; *P. m. turkestanicus* in the extreme northwest; *P. m. minor* in most areas of northern China; *P. m. commixtus* in the south of the Yangtze river; *P. m. subtibetanus* in the mountainous areas of southwest China; *P. m. tibetanus* in the southeastern areas of the Tibetan plateau and *P. m. hainanus* on Hainan Islands (Li et al. 1982) (Fig. 1). According to the subspecies group definition, the first two subspecies belong respectively to the *major* and the *bokharensis* group, the last subspecies belongs to the *cinereus* group and the others belong to the *minor* group (Li et al. 1982).

We here used molecular data and ecological niche models (ENMs) to address the effects of climatic changes on the distribution, divergence and demography of Asian populations of the great tit. Specimens were collected from most of the seven subspecies' range in China. As the first step in clarifying the evolutionary relationships of *P. major*, we attempted to clarify the phylogeny of *P. major* populations in China using maximum likelihood (ML) and Bayesian inference (BI) methods. In addition, divergence times among main clades were estimated using a Bayesian analysis in the software BEAST. We also simulated the historical demography of the main clades in China using a Bayesian skyline plot (BSP) and ENMs. We anticipate that clarifying the divergence pattern and historical dynamics of Asian populations of *P. major* will improve the understanding of the glacial impacts on Asian birds, and also provide a useful basis for future comprehensive studies of the *P. major* complex.

Material and methods

Sample collection, DNA amplification and sequencing

We collected 200 specimens in China (26 sampling sites) and 13 specimens in Mongolia (two sampling sites) from 2003 to 2010 (Fig. 1). All specimens were captured with mist-nets. For each specimen, we visually categorized the subspecies following Li et al. (1982). DNA was extracted from blood or tissue samples using the DNeasy Blood and Tissue Kit (Qiagen, Valencia, CA, USA). To extend our analysis, 112 previously published mitochondrial DNA (mtDNA) control region (CR) sequences were downloaded from GenBank (Supplementary material Appendix 1). These sequences were from western Europe (n = 59), Russia (n = 34), Morocco (n = 1), central Asia (n = 4), Nepal (n = 3), North Korea (n = 2) and Japan (n = 9) (Kvist et al. 2003). We used the same primers and amplification conditions described in Kvist et al. (2003) to sequence the CR gene of the 213 newly collected specimens from China and Mongolia. In addition, we also amplified the cytochrome *c* oxidase subunit I (COI) and NADH dehydrogenase subunit 2 (ND2) genes of all newly collected specimens. The primers L6615 and H7956 were used for the amplification of the COI gene (Gill et al. 2005). PCR reactions were run using the following thermal profile: denaturation at 94°C for 2 min, followed by 40 cycles of 93°C for 30 s, 46°C for 45 s, and 72°C for 1 min, and a final 10 min at 72°C. The ND2 gene was amplified using the primers pairs L5219/H6313 (Sorenson et al. 1999). The thermal profile used for amplification was 2 min at 94°C followed by 40 cycles of 45 s at 93°C, 30 s at 53°C, and 1 min at 72°C, and a final 10 min at 72°C. The PCR products were purified using the QIAquick PCR purification Kit (QIAGEN). Sequencing was carried out using an ABI PRISM 3730 automatic sequencer following the ABI PRISM BigDye Terminator Cycle Sequencing protocol. Both strands of each PCR product were sequenced. Complete sequences were assembled using Seqman II (DNASTAR). Sequences were aligned using Clustal W (Thompson et al. 1994) as implemented in MEGA ver. 4.0 (Tamura et al. 2007). All sequences are accessible at GenBank (accession numbers HM185122-185126, HM185129-183158, HM185161-185163, HM165-167, HM173-177, HQ833106-833134 for CR, HQ833048-833105 for COI and HQ833137-833182 for ND2).

Description of the two mtDNA datasets used in subsequent analysis

The 213 newly determined CR sequences were first analyzed together with the 112 downloaded sequences. A separate dataset based on the 213 newly concatenated sequences was

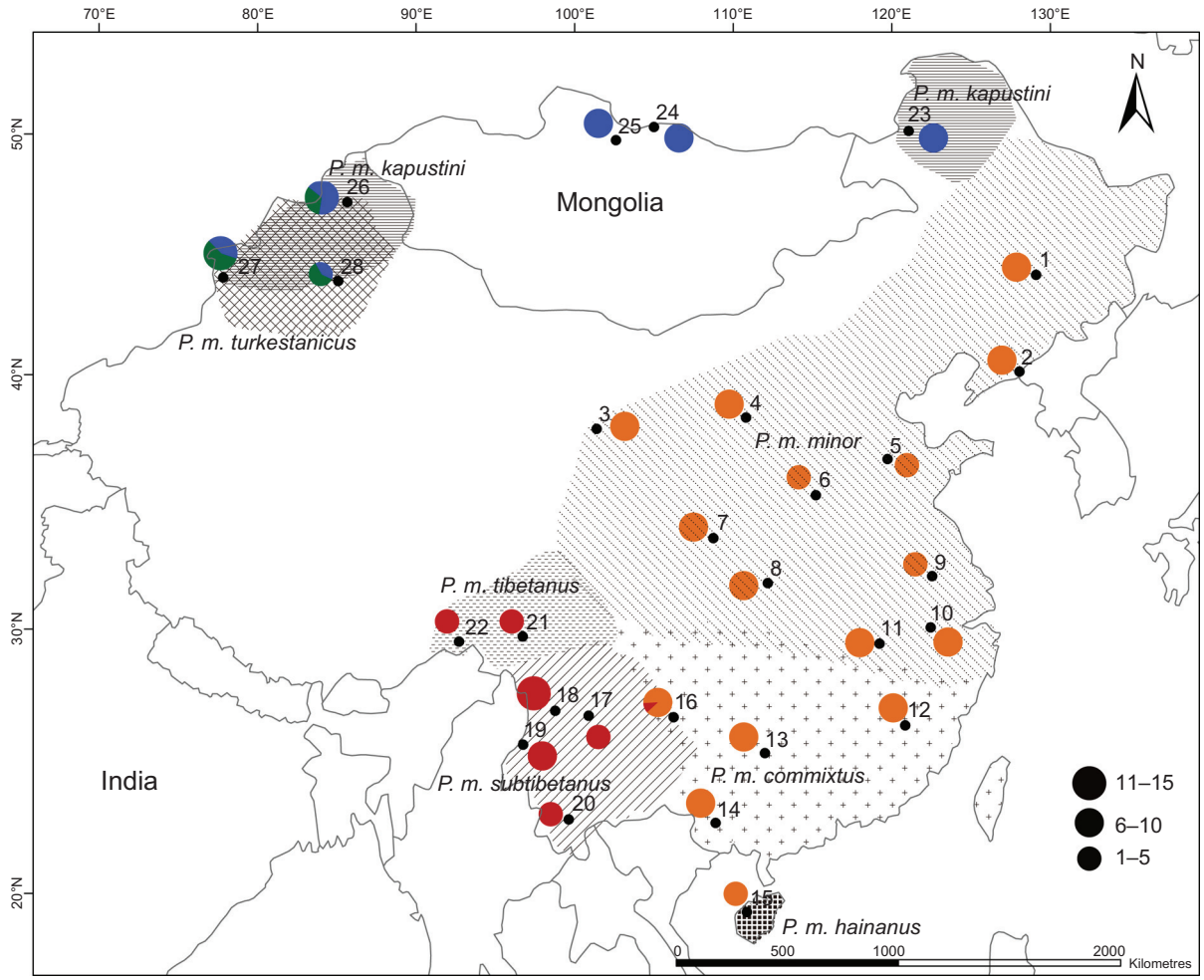

Figure 1. (a) Subspecies distributions of *P. major* in China. (b) Sampling sites are represented by black dots. Locality numbers correspond to those in Table 1: 1, Zuojiazhen; 2, Dandong; 3, Sunan; 4, Yulin; 5, Jinan; 6, Jiaozuo; 7, Foping; 8, Shennongjia; 9, Nanjing; 10, Jixi; 11, Jiujiang; 12, Longxishan; 13, Gulin; 14, Fusui; 15, Nada; 16, Guiding; 17, Yanbian; 18, Lijiang; 19, Gaoligongshan; 20, Puer; 21, Mangkang; 22, Bomi; 23, E'erguna; 24, Tuxg; 25, Txg; 26, Aletai; 27, Yining; 28, Wulumuqi. Sites 24 and 25 are located in Mongolia. (c) Geographical distributions of haplotypes of the four main clades in the present phylogenetic analyses. Haplotypes were generated based on concatenated sequences of ND2 and COI. Size of circles represents the number of samples taken at a particular location and the areas of the circles are proportional to the frequencies of those haplotypes.

prepared to estimate the divergence time and demographic history of Asian populations. Each concatenated sequence includes two partitions: COI from nucleotide 1-1247 and ND2 from nucleotide 1248-2217. Unique haplotypes contained in each of the two datasets were identified using DNASP ver. 4.0 (Rozas et al. 2003).

Neutrality test and genetic diversity

The McDonald–Kreitman (McDonald and Kreitman 1991) test was used to examine the selective neutrality of the two mtDNA protein-coding fragments. Two additional neutrality test, Fu and Li's *D* (Fu and Li 1993) and Fu's *Fs* (Fu 1997) were used to detect departures from the mutation-drift equilibrium that would be indicative of changes in historical demography and natural selection. All three tests were implemented in DNASP. The numbers of haplotypes, haplotype diversity (*h*) and nucleotide diversity (π) of each sampling site, were computed from the concatenated sequence dataset in DNASP.

Molecular phylogenetic reconstruction

Phylogenetic relationships among haplotypes were reconstructed using maximum likelihood (ML) and Bayesian inference (BI). One green-backed tit *Parus monticolus* was used as the outgroup (GenBank accession numbers HQ833135 for CR, HQ833185 for COI and HQ833183 for ND2). Based on the Akaike information criterion (AIC), the model Hasegawa–Kishino–Yano + invariable sites + Gamma (HKY + I + G, $-\ln L = 2407.70$, $K = 6$, AIC = 4827.40) and General time reversible + invariable sites + Gamma (GTR + I + G; $-\ln L = 5167.32$, $K = 10$, AIC = 10354.64) were selected by the software MrModeltest ver. 2.3 (Nylander 2004) for the CR dataset and the concatenated sequences dataset respectively. The ML tree and associated support were obtained from 1000 nonparametric bootstrap pseudoreplicates in the program PHYML ver. 2.4.4 (Guindon and Gascuel 2003). Bayesian phylogeny was implemented in MRBAYES ver. 3.1 (Huelsenbeck and Ronquist 2001). The analysis was

run for 80 million generations or more using three 'heated' and one 'cold' Markov chains with a sampling frequency of 1/1000 trees. In general, the most credible inference of relationship was confined to nodes where the nonparametric bootstrap value (ML) was $\geq 70\%$ and the Bayesian posterior probability (BI) was $\geq 95\%$.

Hierarchical analysis of molecular variance

A hierarchical analysis of molecular variance (AMOVA; Schneider et al. 2000) was performed using Arlequin ver. 3.5 (Excoffier et al. 2005) to test the segregation of genetic variation according to the haplotype clades indicated in the ML and BI results. Our AMOVA analysis estimated the proportion of variation among clades (Φ_{CT}), the proportion of variation among populations within clades (Φ_{SC}) and the proportion of variation within populations (Φ_{ST}). Significance levels were determined by replicating nonparametric procedures 10 000 times. AMOVA was analyzed using the concatenated sequences dataset.

Divergence time estimate

A Bayesian framework in the software BEAST ver. 1.6.1 (Drummond and Rambaut 2007) was used to calculate the divergence time among mitochondrial clades. The uncorrelated lognormal relaxed molecular clock (Drummond et al. 2006) and constant size for the coalescent model were chosen. The analysis was run for 300 million generations, sampling every 30 000 generations. The substitution model was selected according the results obtained by MrModeltest. As no fossil data were available for calibrating substitution rates, we assumed a molecular clock based on the mutation rate of the mitochondrial cytochrome *b* in tits (Paridae) (0.8×10^{-8} site^{-1} yr^{-1}) (Päckert et al. 2007), which is consistent with the Hawaiian honeycreepers' mtDNA clock (Fleischer et al. 1998). The substitution rate for the concatenated sequence alignment was calculated by multiplying the ratio of the net average distance (D_a) for the concatenated sequence against that for cyt *b* alone between *P. major* and the *P. montanus* outgroup. The calculation of D_a was implemented in MEGA using *p*-distances. The net average distance between the two species was 0.044 for concatenated sequences, 1.2 times greater than that estimated from cyt *b* alone. Therefore, a mean substitution rate of 0.96×10^{-8} site^{-1} yr^{-1} for the concatenated sequences was used. Stationarity in BEAST was investigated by examining the effective sample size (ESS), which was > 200 for all estimated parameters.

Historical demography

We reconstructed the past population dynamics of mitochondrial clades of *P. major* using the Bayesian skyline plot (BSP; Drummond et al. 2005) method implemented in BEAST. This genealogical method utilizes Markov chain Monte Carlo (MCMC; Drummond et al. 2002) sampling of sequence data to estimate a posterior distribution of effective population sizes through time. Chains were run for 100 million generations and the first 10% discarded as 'burn-in'. The best substitution model was selected according to MrModeltest. We applied 10 grouped coalescent intervals and constant growth rate for the skyline model. The mutation rate was the same as that used in the divergence time analysis. Demographic history through time was reconstructed using Tracer ver. 1.4 (Rambaut and Drummond 2007).

The exponential growth rate was also estimated for each clade by FLUCTUATE ver. 1.4 (Kuhner et al. 1998). FLUCTUATE was initiated with a Watterson (1975) estimate of theta (Θ), and a random topology, performing 10 short chains, sampling every 20 genealogies for 200 steps, and two long chains, sampling every 20 genealogies for 20 000 steps. FLUCTUATE analyses were repeated five times, and the mean and standard deviation of Θ and '*g*' (population growth parameter) were calculated from the results of these separate runs. However, this genealogical method was known to yield estimates of *g* with an upward bias (Kuhner et al. 1998). Thus, we corrected *g* values following the conservative approach of Lessa et al. (2003) and only considered the *g* value indicative of population growth when $g > 3SD$ (g).

Ecological niche models

Ecological niche models (ENMs) utilize associations between environmental variables and known species' occurrence localities to define abiotic conditions within which populations can be maintained (Guisan and Thuiller 2005). This approach makes it possible to map areas of environmental suitability for a species based on the physical environmental conditions, even when there is very limited locality data on the species distributions (Pearson et al. 2007). This approach has been somewhat controversial because it assumes that information on the distribution of ancestral species at the time of speciation can be deduced from the current distribution of their descendents (Peterson et al. 1999, Martínez-Meyer and Peterson 2006). Nonetheless, integrating phylogeographic and ecological analysis has become more common in recent years, and this approach had provided new insights on species' distribution (Graham et al. 2004, Raxworthy et al. 2007, Rissler and Apodaca 2007, Dai et al. 2011, Flanders et al. 2011). To address if suitable habitat for *P. major* populations in China changed according to glacial fluctuations, we used Maxent ver. 3.3.2 (Phillips and Dudik 2008) to predict suitable distributions during the present and the LGM. Maxent was selected because it has been shown to perform well compared with alternative modeling methods (Elith et al. 2006) and is robust to low sample sizes (Pearson et al. 2007). Presence localities were obtained from our own field surveys and museum records (The National Zoological Museum of China). The environmental data layers for both present and LGM were available from the WorldClim dataset (<www.worldclim.org>) (Hijmans et al. 2005) at 2.5-arcminute resolution, which comprises 19 bioclimatic variables representing annual trends, seasonality and extremes of temperature and precipitation. Some studies have confirmed that the predictions of LGM refugial locations from these environmental data layers and predictions based on traditional phylogeographic analyses were significantly spatially correlated (Carstens and Richards 2007, Waltari

et al. 2007, Vega et al. 2010, Flanders et al. 2011). ENMs were built according to current environmental factors and then projected onto the LGM environmental data layers. The convergence threshold was left at default, the maximum number of iterations was set at 2000 and the fade-by-clamping option was chosen to remove heavily clamped pixels from the prediction. Model performance was evaluated using the area under the curve (AUC) and threshold-dependent binomial omission tests. Values between 0.7–0.9 indicate excellent discrimination (Swets 1988). We modeled the ecological niche 10 times, using a different 80% of localities to train the model and 20% to test the model, and visually compared AUC scores and jackknife tests of variable importance to assess consistency between runs. The maps were imported to ARC GIS 9.3 (ESRI) for final outputs. To further examine whether different mitochondrial clades occupied distinct ecological niche spaces, we also created two 'reduced ENMs' using only localities from the target clade following the procedures above.

Results

Genetic polymorphism

We sequenced 539 bp of the CR gene, 1247 bp of the COI gene, and 970 bp of the ND2 gene for the 213 *P. major* individuals sampled in China and Mongolia. CR alignment of the 213 newly determined and 112 downloaded sequences yielded 122 variable sites (82 were parsimony informative) and 6 insertions or deletions, identifying 123 haplotypes. The 213 newly concatenated sequences contained 178 variable sites of which 132 were parsimony informative, generating 86 haplotypes. The McDonald–Kreitman test showed no significant deviation from neutrality for the two mitochondrial coding segments (Fisher's exact test, $p > 0.05$). Values of Fu and Li's *D* for COI and ND2 were -2.12 and -0.66 respectively, each of which is not statistically significant ($p > 0.05$). For Fu's *Fs*, significance at the 0.05 level was indicated when p values were < 0.02 (Excoffier et al. 2005). Values of the Fu' *Fs* test for COI and ND2 were -2.57 and 0.755 respectively, neither of which is statistically significant ($p > 0.02$). These results indicate that the observed nucleotide polymorphism was selectively neutral. Based on the concatenated sequences, haplotype diversities ranged from 0.286 to 1 and nucleotide diversities ranged from 0.013 to 0.586% for all sampling sites where the sample size was more than three (Table 1).

Phylogeographic pattern

Tree topology based on the CR dataset was similar for the BI and ML analyses, and both consistently separated *P. major* into five distinct clades (labeled A to E in Fig. 2a). Clade A is restricted to east Asia, including Japan, Korea and most of China. Clade B is comprised of haplotypes from mountainous areas of southwest China. According to the current subspecies classification, Clade A and B collectively correspond to the *minor* and part of the *cinereus* group. Clade C includes the Nepalese population and corresponds to the *cinereus* group. Clade D corresponds to the *major* group and occupies a vast area from northwest Africa and Europe to Siberia and Clade E contains the samples from the central Asia and corresponds to the *bokharensis* group. Clades A, B and C in the eastern part of the Himalaya form a superclade which is a sister group to another superclade in the western part of the Himalaya comprised of Clades D and E (Fig. 3). Most clades themselves and the relationships between them were strongly supported by Bayesian probabilities and ML bootstrap values. However the relationship between Clade C and A–B had posterior probabilities of $< 95\%$ and ML bootstrap of $< 70\%$ (Fig. 2a). Tree topology based on the concatenated sequences dataset was compatible to that of the CR dataset, except no Clade C (Fig. 2b). Clade C was not represented on the concatenated sequences tree because it was only found in GenBank samples. Nucleotide diversity of Clade B was higher (0.262%) than that of Clade A, D and E (0.098, 0.078 and 0.053%, respectively). Some populations possessed haplotypes from two clades, including four localities of Yining, Aletai, Wulumuqi and Guiding, which had haplotypes from Clades D/E, D/E, D/E and A/B, respectively (Fig. 1, Table 1). These two molecular phylogenetic tree estimates are far from being monophyletic for subspecies. According to the current subspecies taxonomy, *P. m. minor*, *P. m. commixtus* and *P. m. hainanus* belong to Clade A, Clade B includes *P. m. tibetanus* and *P. m. subtibetanus*, *P. m. kapustini* belongs to Clade D, and *P. m. turkestanicus* corresponds with Clade E.

Hierarchical analysis of molecular variance

The AMOVA with three hierarchical levels assigned 95.90% of the total genetic variance to variation among clades and 3.12% to variation among individuals within populations. When we applied AMOVA to each phylogenetic clade, the percentage of overall variation attributed to variation among populations for Clades A, B and D clade (19.07, 16.80 and 31.94%, respectively) was lower than that attributed to variation among individuals within populations (80.93, 83.20 and 68.06%, respectively). For Clade E, the percentage of overall variation attributed to variation among populations (84.27%) was higher than that attributed to variation among individuals within populations (15.73%).

Divergence time estimate

All divergences within *P. major* estimated by BEAST occurred in the Early–Middle Pleistocene. The first divergence occurred 2.19 (95% HPD: 3.05–1.36) million yr ago (mya) and resulted in the split between the two eastern clades (A and B) and the two western clades (D and E). Subsequently divergences occurring 1.47 (95% HPD: 2.09–0.84) mya resulted in the separation of Clade A and B, which encircle the southeastern and eastern flanks of the Tibetan plateau. The last divergence, the separation of Clade D and E, took place approximately 0.61 (95% HPD: 0.99–0.29) mya.

Table 1. Geographical distributions of *P. major* haplotypes based on the concatenated sequences of ND2 and COI. Shading indicates the putative natural distribution of each clade, corresponding to that shown in Fig. 2. Locality numbers of sampling sites correspond to those in Fig. 1. *h*, haplotype diversity; π, nucleotide diversity.

		h	π (%)	1 Zuojiazhen	2 Dandong	3 Sunan	4 Yulin	5 Jinan	6 Jiaozuo	7 Fuping	8 Shennongjia	9 Nanjing	10 Jixi	11 Jiujiang	12 Longxishan	13 Gulin	14 Fusui	15 Nada	16 Guiding	17 Yanbian	18 Lijiang	19 Gaoligong	20 Puer	21 Mangkang	22 Bomi	23 E'erguna	24 Tuxg	25 Txg	26 Yining	27 Aletai	28 Wulumuqi
		0.370	0.018																											
		0.933	0.134																											
		0.286	0.026																											
		0.667	0.052																											
		1	0.045																											
		1	0.060																											
		0.848	0.112																											
		0.867	0.075																											
		1	0.060																											
		0.933	0.118																											
		0.970	0.142																											
		0.782	0.112																											
		0.533	0.027																											
		0.643	0.084																											
		0	0																											
		0.694	0.586																											
		1	0.217																											
		0.970	0.125																											
		1	0.382																											
		1	0.353																											
		/	/																											
		/	/																											
		0.750	0.106																											
		0.286	0.013																											
		0.333	0.015																											
		0.933/0.255																												
		0.511/0.400																												
		0/0	0/0																											
A	Con1			8	3	6	6	1	1	5	3	1	1	1	2	7	5		2											
	Con2			1																										
	Con3			1																										
	Con4				1																									
	Con5				1																									
	Con6				1																									
	Con7				1																									
	Con8				1		1						1	1																
	Con9				1						1																			
	Con10				1																									
	Con11					1																								
	Con12						1							2																
	Con13						1																							
	Con14						1				1		3	1	1															
	Con15							1																						
	Con16								1																					
	Con17								1	1						1			1											
	Con18									1																				
	Con19									1																				
	Con20									1				1		1														
	Con21									1																				
	Con22									1																				
	Con23									1																				
	Con24										3																			
	Con25										1																			
	Con26										1																			
	Con27											1																		
	Con28											1																		
	Con29												1																	
	Con30												1																	
	Con31												1																	
	Con32												1																	
	Con33												1	1	1															
	Con34													2																
	Con35													1																
	Con36													1																
	Con37													1																
	Con38														2															
	Con39														5															
	Con40															1														
	Con41																1													
	Con42																1													
	Con43																1													
	Con44																	2												
	Con45																		5											
B	Con46																		1											
	Con47																			1										
	Con48																			1	2									
	Con49																			1										
	Con50																			1										
	Con51																			1										
	Con52																				1									
	Con53																				2									
	Con54																				1									
	Con55																				1									
	Con56																				1									
	Con57																				1									
	Con58																				1									
	Con59																				1									
	Con60																				1									
	Con61																					1								
	Con62																					1								
	Con63																					1								
	Con64																					1								
	Con65																					1								
	Con66																					1								
	Con67																						1							
	Con68																						1							
	Con69																						1							
	Con70																						1							
	Con71																							1						
	Con72																								1					
D	Con73																									3	6	5	1	7	
	Con74																									2					
	Con75																									3			2	2	
	Con76																										1				
	Con77																											1			
	Con78																												1		
	Con79																												1		
	Con80																												1		
	Con81																													1	
	Con82																														2
E	Con83																												4		
	Con84																												1		
	Con85																												7		3
	Con86																												1		

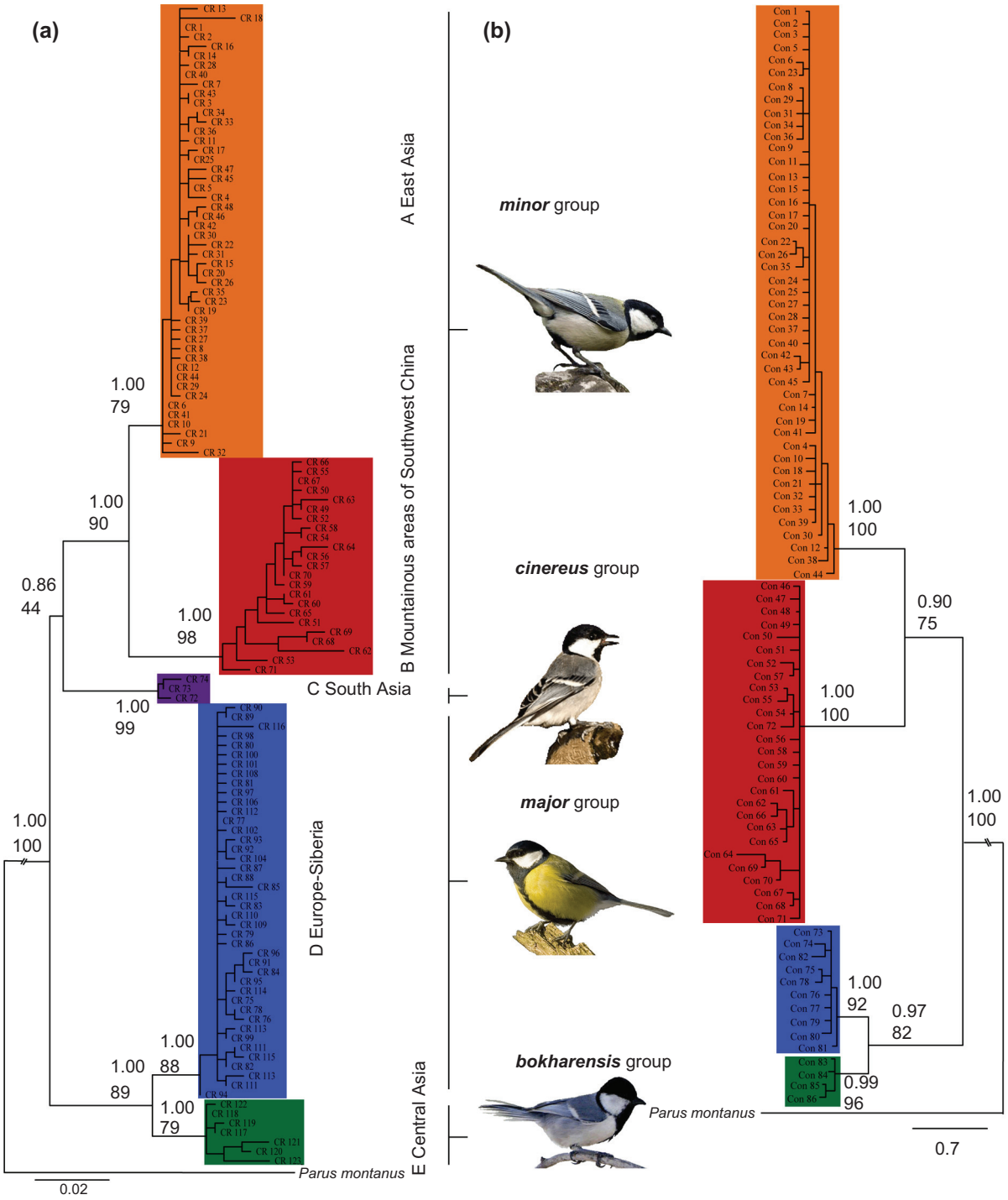

Figure 2. (a) Maximum likelihood (ML) tree based on the haplotypes of the 213 newly determined and 112 previously published CR sequences. (b) ML tree based on haplotypes of the 213 newly determined concatenated sequences. Nodal values above the line indicate bootstrap supports and posterior probabilities of ML/BI. The bootstrap and BI values are given only for the nodes of the main clades. Main clades are indicated by A–E.

Historical demography

The historical population trend inferred by the Bayesian skyline plot showed that Clade A experienced a long period of relative population stability before undergoing an increase about 0.03–0.015 mya, after which it again remained stable until the present (Fig. 4a). The population dynamics of *P. major* in the mountainous areas of southwest China (Clade B) is indicative of continuous growth over 0.13–0.02 mya (Fig. 4b). Clade D appears to have undergone population expansions after the LGM (Fig. 4c). We did not construct BSP for Clade E because of insufficient samples. Recent population growths of the Clade A, B and D were also supported by maximum likelihood estimates of

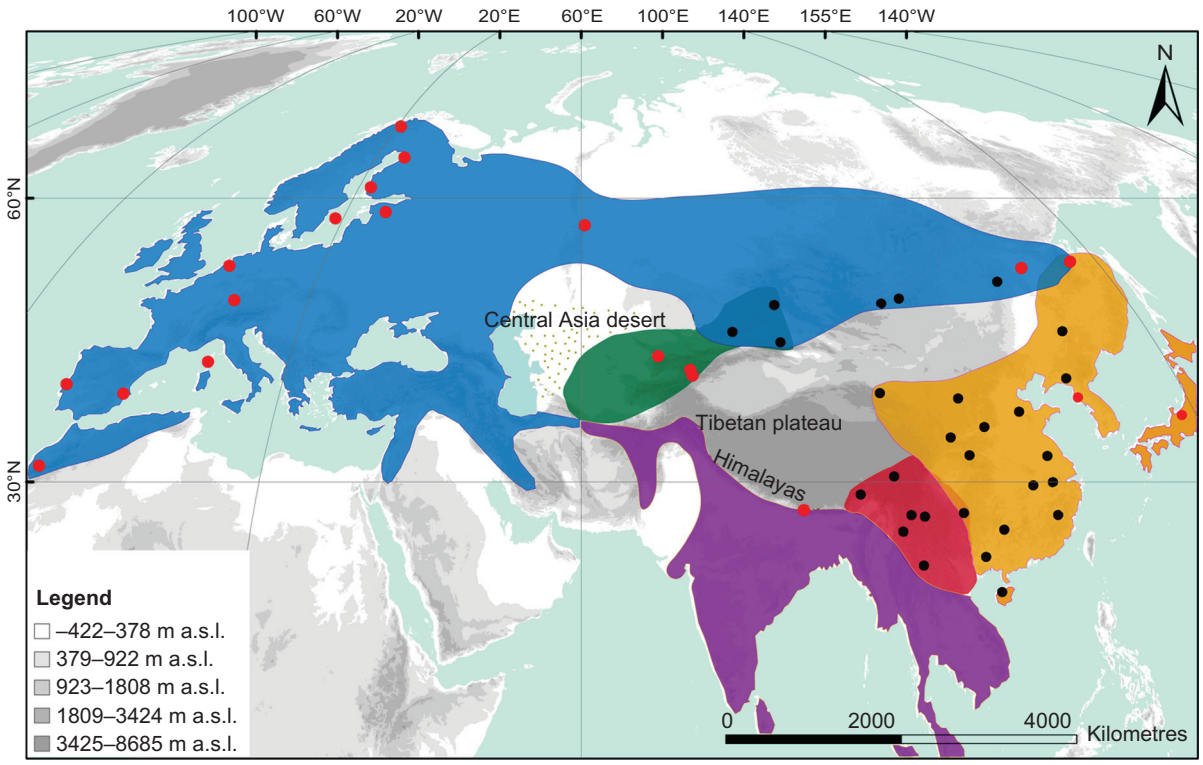

Figure 3. Global geographical distribution of five main clades of *P. major* based on control region (CR) sequences. Black circles represent the locations from which samples were obtained in this study and red circles represent locations from which previously published sequences were obtained. The distribution areas are redrawn after Harrap and Quinn (1996).

the exponential growth rate in FLUCTUATE (positive corrected *g* values: 3360.13 for Clade A, 1741.66 for Clade B and 1858.11 for Clade D).

Ecological niche distributions

Maxent appeared to perform well for the full ENMs, with average test AUC values of 0.859 ± 0.042 SD. Predictions were significantly different from random at all binomial omission test thresholds across all 10 runs. The spatial prediction generated for the present full ENM was largely congruent with our prior expectations for the distribution of *P. major* in China (Fig. 5a). The ENM suggests that the present distribution of *P. major* is similar to its distribution during the LGM (Fig. 5b). The average test AUC values for the two reduced ENMs, averaged across 10 replicate runs, were moderately high (0.832 ± 0.035 SD for Clade A and 0.910 ± 0.079 SD for Clade B), substantially better than that of a random model. These projected distributions for the two reduced ENMs are highly coincident with their phylogeographic ranges (Fig. 5c, d).

Discussion

MtDNA clade divergence pattern

Previous studies suggested that the mitochondrial haplotypes of *P. major* could be divided into four monophyletic clades (Kvist et al. 2003, Zink 2005). However, we found five highly divergent clades (Fig. 2a), including one in the mountainous areas of southwest China that was previously unknown. Phylogenetic inferences indicate that the node support for this clade is high (Fig. 2a, b).

The phylogeny of the haplotypes was not completely consistent with the classification of the four subspecies groups. Previously morphological studies considered that the contact zone between the *minor* and *cinereus* groups was in southern China, specifically an elongated area extending from coastal southeastern China to parts of northern Thailand (Eck and Piechocki 1977, Harrap and Quinn 1996). However, our molecular data indicate that *minor* and *cinereus* in China have a common mitochondrial gene pool. The tree topology supports the view that the *major* and *bokharensis* subspecies groups are monophyletic.

China's extreme northwest is part of the phylogeographic break and secondary contact zone between the *major* and *bokharensis* groups (Formozov et al. 1993, Kvist et al. 2007). *Parus m. kapustini* and *P. m. bokharensis*, which have remarkable morphological and genetic differences, are sympatric in this area (Fig. 1). We observed that the coloration of these subspecies, especially lipochromes of the breast and belly, form a continuous transition from pure *P. m. kapustini* to pure *P. m. bokharensis*, even within a small area. The pure *P. m. kapustini* has a haplotype of Clade D whereas the pure *P. m. bokharensis* haplotype corresponds Clade E. Phenotypically intermediate individuals had haplotypes belonging to Clade D or E. A full resolution analysis of

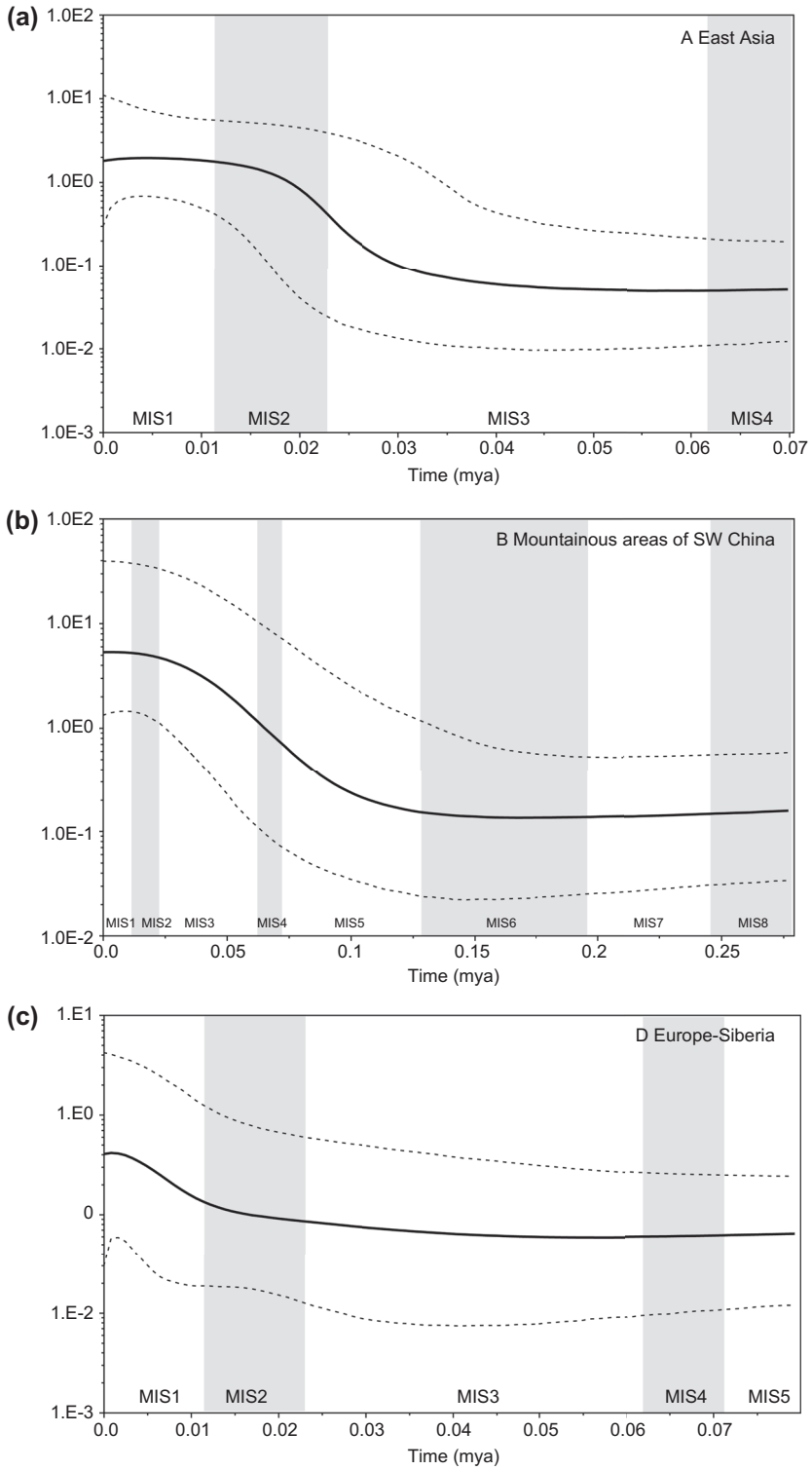

Figure 4. Bayesian skyline plot representing historical demographic trends in the main mitochondrial DNA clades of *P. major*. (a) East Asia clade; (b) mountainous areas of SW China clade; (c) European-Siberian clade. The x axis is in units of millions of years ago and is estimated based on a rate of 0.96×10^{-8} substitutions site^{-1} yr^{-1}. The y axis is equal to $N_f e$ (the product of the effective female population size and the generation time in years (log transformed)). Estimates of means are joined by a solid line while the dashed lines delineate the 95% HPD limits. The abbreviation MIS refers to marine isotope stage.

alleles or microsatellites is required to gain a greater understanding of the hybridization processes. Effects of Pleistocene climate change on population divergence.

Extant *P. majo*r populations are widely distributed in Eurasia encircling the central Asian desert and the Tibetan Plateau. The diversification of *P. major* has occurred on a broad geographic scale across the entire sampling area (Fig. 3). The correlation between phylogeographic breaks and some geographic barriers (e.g. central Asian deserts, the Tibetan plateau and mountains) is strong. Recently,

the uplift of the Tibetan Plateau has been hypothesized to induce phylogeographic breaks within, or among, species in southeast Asia, including species both on and outside of the plateau (Yang et al. 2006, Song et al. 2009). The uplift of the Tibetan plateau had profound effects on the geological environment of the plateau itself and adjacent areas. For examples, the uplift induced a high rate of precipitation on the southern flank of the Himalayas causing vegetation to evolve towards tropical biomes. It also resulted in the formation of mountain ranges in southwest China and facilitated the formation of the modern deserts in central Asia and the Middle East (Ramstein et al. 1997). These geographic and environmental events occurred 55–15 mya (Ramstein et al. 1997, Chung et al. 1998, Tapponnier et al. 2001, Royden et al. 2008) or earlier (Kapp et al. 2007). However, considering that *P. major* is estimated to have diverged in the Early–Middle Pleistocene (2.19–0.61 mya), Pleistocene climatic oscillations are more likely to have been responsible for its present phylogeographic structure. The Earth's climate experienced a series of major ice ages from the Pliocene (2.4 mya) to the present. During these cooler and drier glacial periods, deserts expanded and mountains became glaciated. Because *P. major* is a sedentary, hole nesting bird, it was probably sensitive to changes in woodland cover. Indeed, our data are consistent with expanded dry deserts and steep, glaciated mountains effectively preventing gene flow between separated populations.

Given the long internodes between the first divergence in *P. major* that gave rise to the eastern and western superclades and the subsequent divergence within each superclade, we speculate that population divergence within *P. major* has been the result of a series of staged vicariant events, rather than a simultaneous fragmentation. Multiple cooling and warming events during the Pleistocene probably caused multiple effects of population decrease and expansion during the total time frame of clade divergence. Because of geographic complexity and environmental heterogeneity, different clades may not have diverged at the same time. We think it likely that Pleistocene climate-driven vicariant events were responsible for the genetic isolation of *P. major*.

Region–individual demographic patterns influenced by Pleistocene climate oscillations

Pleistocene climate oscillations had a variety of effects on the geographic distribution and demographic history of regional *P. major* populations. The LGM (0.023–0.018 mya) was considered to be critical in influencing the distribution and population size of many species in Europe and North America (Hewitt 2000, 2004, Avise 2009). Kvist et al. (2003) discovered that the *major* group in Europe experienced an expansion from southern refugia to northern areas, and then from Europe to eastern Siberia following the LGM. In China, the *major* group (Clade D) is found only in the extreme northwest and northeast of the country (Fig. 1 and 3). Compared with the present, the ENM indicates that patches of suitable habitat in these regions were smaller during the LGM (Fig. 5a, b). Congruent with this, the genetic data suggest that the population size of this clade increased after the LGM (Fig. 4c).

In contrast to European *P. major* populations, our results show that the LGM had little impact on the geographic distribution of east Asian populations. This conclusion is supported by both the ENMs and BSP analyses. For example, the ENMs suggest that there was as much suitable environment for Clade A and B during the LGM as there is today (Fig. 5a, b). Congruent with this, the Bayesian skyline plot revealed that east Asian populations (Clades A and B) have been stable from the LGM to the present. Based on the BSP results, these populations underwent expansion before the LGM, beginning in the warmer Marine Isotope Stages 3 (MIS3, 0.062–0.023 mya) or MIS5 (0.128–0.071 mya) periods (Fig. 4a, b). MIS is a timescale that is now widely used to express warm and cool periods in the Quaternary (Ogg et al. 2008). A similar pre-LGM expansion has also been detected in other east Asian bird species (Li et al. 2009, Dai et al. 2011, Qu et al. 2011). This difference of demographic patterns between European and east Asian populations seems to be inevitable. In contrast with Europe, the maximum extent of glacial development in east Asia occurred during MIS6 and MIS4, with ice being restricted during the LGM (MIS2) (Benn and Owen 1998, Zhang et al. 2006, Zhou et al. 2006). Palynological and palaeo-climatic data suggest that the vegetation covering east Asia during the warmer MIS3 and MIS5 was similar to that observed today (Yuan et al. 2004, Yu et al. 2007). Therefore, population sizes in east Asia are likely to have expanded during the warmer MIS3 or MIS5 (Fig. 5a, b).

Within east Asia, the demographic history of populations that breed in the mountains (Clade B) versus on the plain (Clade A) appeared to be different. The smaller the climatic shift, the more probable it is that palaeoendemics survive (Jansson 2003). During cooler periods, glaciations in the southwest mountains of China were restricted to relatively high altitudes (Li et al. 1991, Zhou et al. 2006) and did not affect the lower slopes or valleys (Qu et al. 2011). These relatively mild ecological conditions allowed vegetation and species to persist in this region by shifting their altitudinal range. As predicted, Clade B was found to have had a long independent evolutionary history and to have maintained an increased population size through some ice ages, even during the cooler MIS 4 (Fig. 4b).

A cryptic phylogenetic clade in *P. major*

The mountainous areas of southwest China, like the tropical or subtropical mountains of east Africa (Roy 1997) and the Andes (Garcia-Moreno et al. 1999), are centers of bird speciation and endemism (Lei et al. 2007, Huang et al. 2010). Our data indicate that there is a previously undetected, but distinct, clade, Clade B in this region, a sister group to Clade A. Considering the tree topology, the high support for nodes and AMOVA results (94.71% of variation between Clade A and B), we concluded that there is deep molecular divergence between Clade A and B. Phenotypic studies indicate that individuals of Clade B are, on average, larger than those of Clade A, and that their second outermost rectrices are characterized by the larger white patches (Li et al. 1982). No obvious differences were found between these two clades in other morphological characters. The genetic data indicate that the genetic

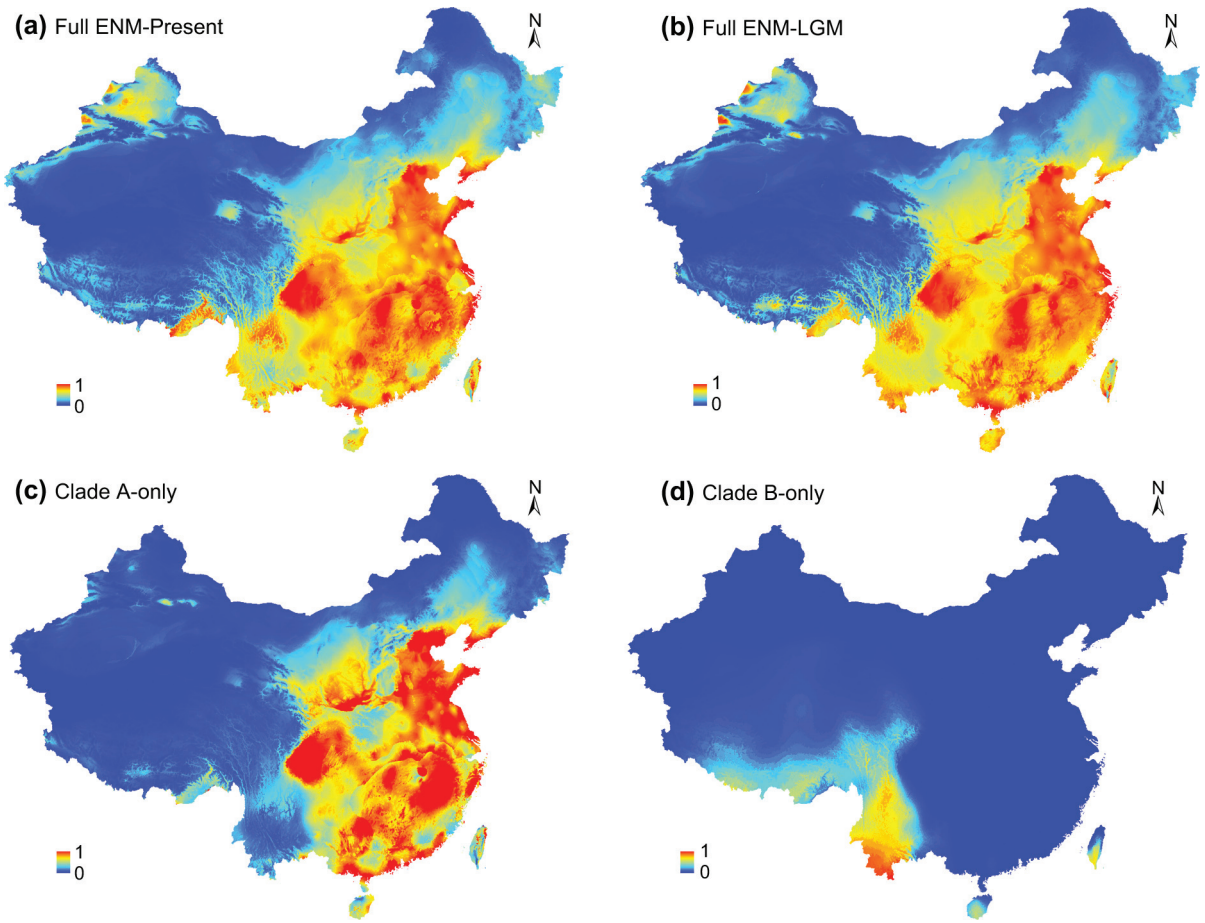

Figure 5. Spatial distribution predictions generated by Maxent. (a) The present distribution of *P. major* in China. (b) The distribution of *P. major* in China during the LGM. (c) The present distribution of Clade A and (d) the present distribution of Clade B. Levels of shading represent continuous logistic probabilities of bioclimatic suitability, corresponding to highest suitability (red) to unsuitable (blue) habitat.

distances (p-distance) between Clade A and B is 2.3%, whereas the distance between Clade D and E is only 0.9%. Some authors treat the *bokharensis* group (Clade D) as a separate species (Li et al. 1982). Others regard these four groups as four separate species (or phylogenetic species) (Stepanyan 1990, Kvist et al. 2003). We think that Clade B could be considered as an independent phylogenetic species because of its greater genetic separation from other clades. Species delimitation can be especially difficult in organisms with cryptic morphological characters and fine-scaled endemism patterns. Although most species or subspecies have been identified using morphological data, our results are further evidence that genetic data can lead to the discovery of previously unknown cryptic clades or species. According to the ecological niche model, which is especially sensitive for detecting recent parapatric speciation driven by ecological divergence, we find that the patterns of divergence in the ecological niche between these two clades to be strongly associated with genetic divergence. ENM results showed that the distributions of Clade A and B have clear ecological and geographic limits (Fig. 5c, d). This suggests that these two clades are physiologically constrained from expanding further to opposite sides. In other words, the current range of each genetic clade contains unique niche information. Via the long-term field surveys, we acknowledge that there could be very limited suitable habitat in their potential contact zone, but to date (2011), no records are known. In addition, because the neighboring Clade C is only represented by three specimens from Nepal and Clade B is close to China' southwestern border, we still cannot determine the exact limits of these clades' distributions. To confirm this, more thorough sampling, especially from Southeast Asia, is required. The taxonomic status of the Clade B would also need to be tested with nuclear DNA and morphological analyses.

The limitation of mtDNA markers

In this study, we used a single mtDNA-only marker, which contains limited information with which to describe population history (Edwards et al. 2005). Many popular phylogeographic methods, especially those that focus appropriately on estimating population parameters rather than those of genes, are known to deliver more accurate and reliable estimates with multiple than with single loci (Edwards and Beerli 2000, Hey and Nielsen 2004, Maddison and Knowles 2006). Even when such methods are focused solely on identifying patterns, multiple genes invariably provide a more accurate indication of population boundaries and numbers than mtDNA alone (Brumfield

et al. 2003). However, an mtDNA-only analysis is a strong first step (Edwards and Bensch 2009) and mtDNA markers can provide the reliable information for detecting the independently evolving groups (Zink and Barrowclough 2008). Resolving more detailed aspects of the phylogeographic process, such as gene flow and speciation itself, will require the analysis of multiple loci.

Conclusions

Our results indicate that *P. major* is comprised of at least five highly divergent clades, including a previously unknown, cryptic clade in the mountainous areas of southwest China. A series of vicariant events in *P. major* were dated to the Early–Middle Pleistocene (2.19–0.61 mya). In contrast to the post-LGM expansion of European populations, all *P. major* clades in east Asia experienced population expansion before the LGM. Pleistocene climate-driven environmental change was not only the primary drivers of divergence in *P. major*, but also shaped its demography and the modern distribution of east Asian populations.

Acknowledgements – We are grateful to many people who assisted with field work or provided specimens including: Zuohua Yin, Xuebin Gao, Bin Gao, Ming Ma and Yuchun Wu. We are especially grateful to Yuning Lai, Xiaobo Zhuang, Zhongxi Chai and La Duo for their help in accessing field sites including those in Xinjiang and Xizang. We owe many thanks to Shou-Hsien Li and Dexing Zhang for their early discussion on this research. This research was supported by grants to Fumin Lei from the Major International (Regional) Joint Research Project (no. 31010103901), the Knowledge Innovation Program of the Chinese Academy of Sciences (KSCX2-EW-J-2), the National Science Fund for Distinguished Young Scientists (no. 30925008) and the Key Laboratory of the Zoological Systematics and Evolution of the Chinese Academy of Sciences (no. O529YX5105). NZ and CD contributed equally to this work.

References

Avise, J. C. 2000. Phylogeography: the history and formation of species. – Harvard Univ. Press.

Avise, J. C. 2009. Phylogeography: retrospect and prospect. – J. Biogeogr. 36: 3–15.

Benn, D. I. and Owen, L. A. 1998. The role of the Indian summer monsoon and the mid-latitude westerlies in Himalayan glaciation: review and speculative discussion. – J. Geol. Soc. 155: 353–363.

Brumfield, R. T., Beerli, P., Nickerson, D. A. and Edwards, S. V. 2003. The utility of single nucleotide polymorphisms in inferences of population history. – Trends Ecol. Evol. 18: 249–256.

Carstens, B. C. and Richards, C. L. 2007. Integrating coalescent and ecological niche modeling in comparative phylogeography. – Evolution 61: 1439–1454.

Chung, S. L., Lo, C. H., Lee, T. Y., Zhang, Y. Q., Xie, Y. W., Li, X. H., Wang, K. L. and Wang, P. L. 1998. Diachronous uplift of the Tibetan plateau starting 40 myr ago. – Nature 394: 769–773.

Dai, C. Y., Zhao, N., Wang, W. J., Lin, C. T., Gao, B., Yang, X. J., Zhang, Z. W. and Lei, F. M. 2011. Profound climatic effects on two east Asian black-throated tits (Ave: Aegithalidae), revealed by ecological niche models and phylogeographic analysis. – PLoS One 6: e29329.

Drummond, A. J. and Rambaut, A. 2007. BEAST: Bayesian evolutionary analysis by sampling trees. – BMC Evol. Biol. 7: 214.

Drummond, A. J., Nicholls, G. K., Rodrigo, A. G. and Solomon, W. 2002. Estimating mutation parameters, population history and genealogy simultaneously from temporally spaced sequence data. – Genetics 161: 1307–1320.

Drummond, A. J., Rambaut, A., Shapiro, B. and Pybus, O. G. 2005. Bayesian coalescent inference of past population dynamics from molecular sequences. – Mol. Biol. Evol. 22: 1185–1192.

Drummond, A. J., Ho, S. Y. W., Phillips, M. J. and Rambaut, A. 2006. Relaxed phylogenetics and dating with confidence. – PLoS Biol. 4: e88.

Eck, S. and Piechocki, R. 1977. Eine Kontaktzone zwischen den *bokharensis*-Subspezies und den *major*-Subspezies der Kohlmeise, *Parus major*, in der Südwest-Mongolei. – Ann. Ornithol. 1: 127–136.

Eck, S. and Martens, J. 2006. Review of the Aegithalidae ets. – Zool. Med. Leiden 80: 31–40.

Edwards, S. V. and Beerli, P. 2000. Perspective: gene divergence, population divergence, and the variance in coalescence time in phylogeographic studies. – Evolution 54: 1839–1854.

Edwards, S. V. and Bensch, S. 2009. Looking forwards or looking backwards in avian phylogeography? A comment on Zink and Barrowclough 2008. – Mol. Ecol. 18: 2930–2933.

Edwards, S. V., Kingan, S. B., Calkins, J. D., Balakrishnan, C. N., Jennings, W. B., Swanson, W. J. and Sorenson, M. D. 2005. Speciation in birds: genes, geography, and sexual selection. – Proc. Natl Acad. Sci. USA 102: 6550–6557.

Elith, J., Graham, C. H., Anderson, R. P., Dudik, M., Ferrier, S., Guisan, A., Hijmans, R. J., Huettmann, F., Leathwick, J. R., Lehmann, A., Li, J., Lohmann, L. G., Loiselle, B. A., Manion, G., Moritz, C., Nakamura, M., Nakazawa, Y., Overton, J. M., Peterson, A. T., Phillips, S. J., Richardson, K., Scachetti-Pereira, R., Schapire, R. E., Soberon, J., Williams, S., Wisz, M. S. and Zimmermann, N. E. 2006. Novel methods improve prediction of species' distributions from occurrence data. – Ecography 29: 129–151.

Excoffier, L., Laval, G. and Schneiser, S. 2005. Arlequin (version 3.0): an integrated software package for population genetics data analysis. – Evol. Bioinform. Online 1: 47–50.

Flanders, J., Wei, L., Rossiter, S. J. and Zhang, S. 2011. Identifying the effects of the Pleistocene on the greater horseshoe bat, *Rhinolophus ferrumequinum*, in east Asia using ecological niche modeling and phylogenetic analyses. – J. Biogeogr. 38: 439–452.

Fleischer, R. C., Mcintosh, C. E. and Tarr, C. L. 1998. Evolution on a volcanic conveyor belt: using phylogeographic reconstructions and K-Ar-based ages of the Hawaiian Islands to estimate molecular evolutionary rates. – Mol. Ecol. 7: 533–545.

Formozov, N. A., Keimov, A. B. and Lopantin, V. V. 1993. New hybridization zone of the great titmouse and *Parus bokharensis* in Kazakhstan and relationships in forms of *Parus major* superspecies. – In: Rossomolino, O. L. (eds), Hybridizaion and the problem of species in vertebrates. Archives of the Zoological Museum, Moscow State Univ., pp. 118–146.

Fu, Y. X. 1997. Statistical tests of neutrality of mutations against population growth, hitchhiking and background selection. – Genetics 147: 915–925.

Fu, Y. X. and Li, W. H. 1993. Statistical tests of neutrality of mutations. – Genetics 133: 693–709.

Garcia-Moreno, J., Arctander, P. and Fjeldsa, J. 1999. A case of rapid diversification in the neotropics: phylogenetic relationships among Cranioleuca spinetails (Aves, Furnariidae). – Mol. Phylogenet. Evol. 12: 273–281.

Gill, F. B., Slikas, B. and Sheldon, F. H. 2005. Phylogeny of titmice (Paridae): II. Species relationships based on sequences of the mitochondrial cytochrome-b gene. – Auk 122: 121–143.

Graham, C. H., Ron, S. R., Santos, J. C., Schneider, C. J. and Moritz, C. 2004. Integrating phylogenetics and environmental niche models to explore speciation mechanisms in dendrobatid frogs. – Evolution 58: 1781–1793.

Guindon, S. and Gascuel, O. 2003. A simple, fast, and accurate algorithm to estimate large phylogenies by maximum likelihood. – Syst. Biol. 52: 696–704.

Guisan, A. and Thuiller, W. 2005. Predicting species distribution: offering more than simple habitat models. – Ecol. Lett. 8: 993–1009.

Harrap, S. and Quinn, D. 1996. Tits, nuthatches and treecreepers. – Christopher Helm.

Hewitt, G. M. 1996. Some genetic consequences of ice ages, and their role in divergence and speciation. – Biol. J. Linn. Soc. 58: 247–276.

Hewitt, G. M. 2000. The genetic legacy of the Quaternary ice ages. – Nature 405: 907–913.

Hewitt, G. M. 2004. Genetic consequences of climatic oscillations in the Quaternary. – Phil. Trans. R. Soc. B 359: 183–195.

Hey, J. and Nielsen, R. 2004. Multilocus methods for estimating population sizes, migration rates and divergence time, with applications to the divergence of *Drosophila pseudoobscura* and *D. persimilis*. – Genetics 167: 747–760.

Hijmans, R. J., Cameron, S. E., Parra, J. L., Jones, P. G. and Jarves, A. 2005. Very high resolution interpolated climate surfaces for global land areas. – Int. J. Climatol. 25: 1965–1978.

Huang, X. L., Qiao, G. X. and Lei, F. M. 2010. Use of parsimony analysis to identify areas of endemism of Chinese birds: implications for conservation and biogeography. – Int. J. Mol. Sci. 11: 2097–2108.

Huelsenbeck, J. P. and Ronquist, F. 2001. MRBAYES: Bayesian inference of phylogeny. – Bioinformatics 17: 754–755.

Jansson, R. 2003. Global patterns of endemism explained by past climatic change. – Proc. R. Soc. B 270: 583–590.

Johansson, U. S., Alström, P., Olsson, U., Ericson, P. G. R., Sundberg, P. and Price, T. D. 2007. Build-up of the Himalayan avifauna through immigration: a biogeographical analysis of the Phylloscopus and Seicercus carblers. – Evolution 61: 324–333.

Kapp, P., Decelles, P. G., Gehrels, G. E., Heizier, M. and Ding, L. 2007. Geological records of the Lhasa-Qiangtang and Indo-Asian collisions in the Nima area of central Tibet. – Geol. Soc. Am. Bull. 119: 917–932.

Kuhner, M., Yamato, J. and Felsenstein, J. 1998. Maximum likelihood estimation of population growth rates based on the coalescent. – Genetics 149: 429–434.

Kvist, L., Martens, J., Higuchi, H., Nazarenko, A. A., Valchuk, O. P. and Orell, M. 2003. Evolution and genetic structure of the great tit (*Parus major*) complex. – Proc. R. Soc. B 270: 1447–1454.

Kvist, L., Arbabi, T., Päckert, M., Orell, M. and Martens, J. 2007. Population differentiation in the marginal populations of the great tit (Paridae: *Parus major*). – Biol. J. Linn. Soc. 90: 201–210.

Lei, F. M., Wei, G. A., Zhao, H. F., Yin, Z. H. and Lu, J. L. 2007. China subregional avian endemism and biodiversity conservation. – Biodivers. Conserv. 16: 1119–1130.

Lessa, E. P., Cook, J. A. and Patton, J. L. 2003. Genetic footprints of demographic expansion in North America, but not Amazonia, during the Late Quaternary. – Proc. Natl Acad. Sci. USA 100: 10331–10334.

Li, G. Y., Zheng, B. L. and Liu, G. Z. 1982. Passeriformes. – Fauna Sinica, Aves. Vol. 13. Science Press, Beijing.

Li, S. H., Yeung, C. K. L., Feinstein, J., Han, L., Le, M. H., Wang, C. X. and Ding, P. 2009. Sailing through the Late Pleistocene: unusual historical demography of an east Asian endemic, the Chinese hwamei (*Leucodioptron canorum canorum*), during the last glacial period. – Mol. Ecol. 18: 622–633.

Li, Z. W., Chen, Z. R. and Wang, M. L. 1991. Classification and correlation of the quaternary glacial epoch in the Hengduan (Transverse) Mountains. – Geol. Rev. 37: 125–132.

Liu, Y., Zhan, X. J., Wang, N., Chang, J. and Zhang, Z. W. 2010. Effect of geological vicariance on mitochondrial DNA differentiation in common pheasant populations of the Loess Plateau and eastern China. – Mol. Phylogenet. Evol. 55: 409–417.

Maddison, W. P. and Knowles, L. L. 2006. Inferring phylogeny despite incomplete lineage sorting. – Syst. Biol. 55: 21–30.

Martínez-Meyer, E. and Peterson, A. 2006. Conservatism of ecological niche characteristics in North American plant species over the Pleistocene-to-Recent transition. – J. Biogeogr. 33: 1779–1789.

McDonald, J. H. and Kreitman, M. 1991. Adaption protein evolution at the Adh locus in Drosophila. – Nature 351: 652–654.

Nylander, J. A. A. 2004. MrModeltest v2. – Program distributed by the author, Evolutionary Biology Centre, Uppsala Univ.

Ogg, J. M., Ogg, G. and Gradstein, F. M. 2008. The concise geologic time scale. – Cambridge Univ. Press.

Päckert, M., Martens, J., Eck, S., Nazarenko, A. A., Valchuk, O. P., Petri, B. and Veith, M. 2005. The great tit (*Parus major*) – a misclassified ring species. – Biol. J. Linn. Soc. 86: 153–174.

Päckert, M., Martens, J., Tietze, D. T., Dietzen, C., Wink, M. and Kvist, L. 2007. Calibration of a molecular clock in tits (Paridae) – do nucleotide substitution rates of mitochondrial genes deviate from the 2% rule? – Mol. Phylogenet. Evol. 44: 1–14.

Patriat, P. and Achache, J. 1984. India Eurasia collision chronology has implications for crustal shortening and driving mechanism of plates. – Nature 311: 615–621.

Pavlova, A., Rohwer, S., Drovetski, S. V. and Zink, R. M. 2006. Different post-pleistocene histories of Eurasian parids. – J. Hered. 97: 389–402.

Pearson, R. G., Raxworthy, C. J., Nakamura, M. and Peterson, A. T. 2007. Predicting species distributions from small numbers of occurrence records: a test case using cryptic geckos in Madagascar. – J. Biogeogr. 34: 102–117.

Peterson, A., Sober, J. and Sanchez-Cordero, V. 1999. Conservatism of ecological niches in evolutionary time. – Science 285: 1265–1267.

Phillips, S. J. and Dudik, M. 2008. Modeling of species distributions with Maxent: new extensions and a comprehensive evaluation. – Ecography 31: 161–175.

Qu, Y. H. and Lei, F. M. 2009. Comparative phylogeography of two endemic birds of the Tibetan plateau, the white-rumped snow finch (*Onychostruthus taczanowskii*) and the Hume's ground tit (*Pseudopodoces humilis*). – Mol. Phylogenet. Evol. 51: 312–326.

Qu, Y. H., Luo, X., Zhang, R. Y., Song, G., Zou, F. S. and Lei, F. M. 2011. Lineage diversification and historical demography of a montane bird *Garrulax elliotii* – implications for the Pleistocene evolutionary history of the eastern Himalaya. – BMC Evol. Biol. 11: 174.

Rambaut, A. and Drummond, A. J. 2007. Tracer v1.4. – <http://beast.bio.ed.ac.uk/tracerl>.

Ramstein, G., Fluteau, F., Besse, J. and Joussaume, S. 1997. Effect of orogeny, plate motion and land sea distribution on Eurasian climate change over the past 30 million years. – Nature 386: 788–795.

Raxworthy, C., Ingram, C., Rabibisoa, N. and Pearson, R. 2007. Applications of ecological niche modeling for species delimitation: a review and empirical evaluation using day geckos (*Phelsuma*) from Madagascar. – Syst. Biol. 56: 907.

Rissler, L. and Apodaca, J. 2007. Adding more ecology into species delimitation: ecological niche models and phylogeography

help define cryptic species in the black salamander (*Aneides flavipunctatus*). – Syst. Biol. 56: 924–942.
Roy, M. S. 1997. Recent diversification in African greenbuls (Pycnonotidae: *Andropadus*) supports a montane speciation model. – Proc. R. Soc. B 264: 1337–1344.
Royden, L. H., Burchfiel, B. C. and Van Der Hilst, R. D. 2008. The geological evolution of the Tibetan plateau. – Science 321: 1054–1058.
Rozas, J., Sanchez-Delbarrio, J. C., Messeguer, X. and Rozas, R. 2003. DnaSP, DNA polymorphism analyses by the coalescent and other methods. – Bioinformatics 19: 2496–2497.
Schneider, S., Roessli, D. and Excoffier, L. 2000. Arlequin: a software for population genetics data analysis user manual ver. 2.000. – Genetics and Biometry Lab, Dept of Anthropology, Univ. of Geneva, Geneva.
Song, G., Qu, Y. H., Yin, Z. H., Li, S. S., Liu, N. F. and Lei, F. M. 2009. Phylogeography of the *Alcippe morrisonia* (Aves: Timaliidae): long population history beyond late Pleistocene glaciations. – BMC Evol. Biol. 9: 143.
Sorenson, M. D., Ast, J. C., Dimcheff, D. E., Yuri, T. and Mindell, D. P. 1999. Primers for a PCR-based approach to mitochondrial genome sequencing in birds and other vertebrates. – Mol. Phylogenet. Evol. 12: 105–114.
Stegmann, B. 1931. Die Vögel des dauro-mandschurischen Uebergangsgebietes (Schluß). – J. Ornithol. 79: 137–236.
Stepanyan, L. S. 1990. Conspectus of the ornithological fauna of the USSR. – Nauka, Moscow, Russia.
Swets, J. A. 1988. Measuring the accuracy of diagnostic systems. – Science 240: 1285–1293.
Taberlet, P., Fumagalli, L., Wust-Saucy, A. G. and Cosson, J. F. 1998. Comparative phylogeography and postglacial colonization routes in Europe. – Mol. Ecol. 7: 453–464.
Tamura, K., Dudley, J., Nei, M. and Kumar, S. 2007. MEGA4: molecular evolutionary genetics analysis (MEGA) software version 4.0. – Mol. Biol. Evol. 24: 1596–1599.
Tapponnier, P., Xu, Z. Q., Roger, F., Meyer, B., Arnaud, N., Wittlinger, G. and Yang, J. S. 2001. Geology – oblique stepwise rise and growth of the Tibet plateau. – Science 294: 1671–1677.
Thompson, J. D., Higgins, D. G. and Gibson, T. J. 1994. Clustal W: improving the sensitivity of progressive multiple sequence alignment through sequence weighting, position-specific gap penalties and weight matrix choice. – Nucl. Acids Res. 22: 4673–4680.
Vega, R., Fløjgaard, C., Lira-Noriega, A., Nakazawa, Y., Svenning, J. C. and Searle, J. B. 2010. Northern glacial refugia for the pygmy shrew *Sorex minutus* in Europe revealed by phylogeographic analyses and species distribution modelling. – Ecography 33: 260–271.
Waltari, E., Hijmans, R. J., Peterson, A. T., Nyári, Á. S., Perkins, S. L. and Guralnick, R. P. 2007. Locating pleistocene refugia: comparing phylogeographic and ecological niche model predictions. – PLoS One 2: e563.
Watterson, G. A. 1975. On the number of segregating sites in genetic models without recombination. – Theor. Popul. Biol. 7: 256–276.
Weaver, A. J., Eby, M., Augustus, F. F. and Wiebe, E. C. 1998. Simulated influence of carbon dioxide, orbital forcing and ice sheets on the climate of the Last Glacial Maximum. – Nature 394: 847–853.
Williams, M. A. J., Dunkerley, D. L., De Deckker, P., Kershaw, A. P. and Chappel, J. 1998. Quaternary environments. – Arnold.
Yang, S. J., Yin, Z. H., Ma, X. M. and Lei, F. M. 2006. Phylogeography of ground tit (*Pseudopodoces humilis*) based on mtDNA: evidence of past fragmentation on the Tibetan Plateau. – Mol. Phylogenet. Evol. 41: 257–265.
Yu, G., Gui, F., Shi, Y. and Zheng, Y. 2007. Late marine isotope stage 3 palaeoclimate for east Asia: a data-model comparison. – Palaeogeogr. Palaeoclim. 250: 167–183.
Yuan, D. X., Cheng, H., Edwards, R. L., Dykoski, C. A., Kelly, M. J., Zhang, M. L., Qing, J. M., Lin, Y. S., Wang, Y. J., Wu, J. Y., Dorale, J. A., An, Z. S. and Cai, Y. J. 2004. Timing, duration, and transitions of the Last Interglacial Asian Monsoon. – Science 304: 575–578.
Zhang, W., Cui, Z. J. and Li, Y. H. 2006. Review of the timing and extent of glaciers during the last glacial cycle in the bordering mountains of Tibet and in east Asia. – Quat. Int. 154: 32–43.
Zhou, S. Z., Wang, X. L., Wang, J. and Xu, L. B. 2006. A preliminary study on timing of the oldest Pleistocene glaciation in Qinghai-Tibetan Plateau. – Quat. Int. 154: 44–51.
Zink, R. M. 2005. Natural selection on mitochondrial DNA in *Parus* and its relevance for phylogeographic studies. – Proc. R. Soc. B 272: 71–78.
Zink, R. M. and Barrowclough, G. F. 2008. Mitochondrial DNA under siege in avian phylogeography. – Mol. Ecol. 17: 2107–2121.
Zou, F. S., Lim, H. C., Marks, B. D., Moyle, R. G. and Sheldon, F. H. 2007. Molecular phylogenetic analysis of the grey-cheeked fulvetta (*Alcippe morrisonia*) of China and Indochina: a case of remarkable genetic divergence in a 'species'. – Mol. Phylogenet. Evol. 44: 165–174.

Supplementary material (Appendix J5474 at <www.oikosoffice.lu.se/appendix>). Appendix 1.